Polymer 51 (2010) 2849–2856

Contents lists available at ScienceDirect

Polymer

journal homepage: www.elsevier.com/locate/polymer

# Photoinduced reorientation and polarization holography in photo-cross-linkable liquid crystalline polymer films with large birefringence

Nobuhiro Kawatsuki [a,*], Ayumi Yamashita [a], Mizuho Kondo [a], Taro Matsumoto [b], Tatsutoshi Shioda [b], Akira Emoto [b], Hiroshi Ono [b]

[a] Department of Materials Science and Chemistry, Graduate School of Engineering, University of Hyogo, 2167 Shosha, Himeji 671-2280, Japan
[b] Department of Electrical Engineering, Nagaoka University of Technology, 1603-1 Kamitomioka, Nagaoka 940-2188, Japan

ARTICLE INFO

*Article history:*
Received 5 January 2010
Received in revised form
6 April 2010
Accepted 20 April 2010
Available online 28 April 2010

*Keywords:*
Polymer liquid crystal
Photoinduced orientation
Birefringent film

ABSTRACT

A new photo-cross-linkable liquid crystalline polymer (PLCP) comprised 4-methoxycinnamoyloxy groups connected with a bistolane side group was synthesized to investigate thermally enhanced photoinduced molecular reorientation of a thin film with linearly polarized (LP) 365 nm light exposure. Due to the axis-selective photoreaction of the cinnamate groups followed by the thermally induced self-organization, large molecular reorientation parallel to the polarization of LPUV light ($S > 0.6$) and large birefringence at the non-resonance region ($\Delta n = 0.34$ at 632.8 nm) were obtained. The obtained $\Delta n$ value is the largest among transparent PLCPs in the visible region. The influence of the degree of photoreaction and the annealing temperature on the thermally enhanced molecular reorientation behavior was explored in detail. Finally, for an application of thin optical devices using the PLCP films, pure polarization holographic gratings with large birefringence, which showed periodic molecularly oriented structure, were fabricated using a 325 nm He–Cd laser in various polarization modes and characterized their optical properties.



## 1. Introduction

Much attention has been paid to the photoinduced molecular reorientation of photoreactive polymeric materials due to large number of their applications, such as optical and holographic memories, birefringent optical devices and photoalignment layers for liquid crystal displays [1–8]. Several types of photoreactive polymers, including azobenzene-containing polymers [2–4,9–12] and photo-cross-linkable liquid crystalline polymers (PLCPs) with cinnamate or coumarin end groups [5,6,13–16], have been investigated. New approach for the photoinduced molecular reorientation includes the polymers based on the ionic self-assembly that exhibited very large molecular orientation. [17] The axis-selective photoreaction of these polymeric films was initiated by the use of linearly polarized (LP) light irradiation [18]. For the azobenzene-containing polymers, molecular reorientation perpendicular to the polarization (**E**) of the LP light occurs simultaneously via the axis-selective *trans-cis-trans* photoisomerization process [2]. However, azobenzene-containing polymeric materials are not utilized for display applications because they are colored in the visible region. In contrast, thermally enhanced molecular reorientation parallel to **E** after the axis-selective photoreaction occurs in the cinnamate-containing PLCP films due to the LC characteristics of the material, which causes self-organization [6]. The selectively photoreacted groups parallel to the polarization of the LP light act as a photo-cross-linked anchor to thermally reorient the non-reacted mesogenic groups along them [6,14]. Since the reoriented PLCP films are transparent in the visible region they are useful for display applications [19,20]. To attain thinner molecularly reoriented optical devices, we need larger photoinduced optical birefringence. Therefore, both an efficient molecular orientation and a large inherent birefringence are necessary for useful materials.

Since the tolane moiety has a larger inherent optical birefringence than a biphenyl or phenyl benzoate mesogenic core in LC materials, several types of tolane-containing LC monomers and polymers have been investigated [21–31]. Copolymerization of monomers with tolane side groups is an effective technique for enhancing photoinduced optical anisotropy, where cooperative molecular reorientation is needed [24b,25,27]. Ikeda's group has synthesized azobenzene-containing polymethacrylates copolymerized with monomers containing tolane side groups, which

* Corresponding author. Tel.: +81 79 267 4886; fax: +81 79 267 4885.
*E-mail address:* kawatuki@eng.u-hyogo.ac.jp (N. Kawatsuki).

0032-3861/$ – see front matter © 2010 Elsevier Ltd. All rights reserved.
doi:10.1016/j.polymer.2010.04.043

showed large birefringence [25]. They also reported large photoinduced birefringence in polymethacrylates with a tolane moiety directly attached to azobenzene side groups [23,24]. We have investigated the thermally enhanced photoinduced reorientation behavior in polymethacrylate films consisting of a 4-methoxycinnamoyloxy group connected with a tolane moiety (**P2** in Fig. 1) [28]. This PLCP film showed a larger thermally enhanced photoinduced birefringence ($\Delta n = 0.27$) than that of a polymethacrylate with a biphenyl moiety (**P3** in Fig. 1, $\Delta n = 0.24$). Furthermore, it is known that the bistolane moiety possesses higher inherent birefringence than the tolane moiety. Okano et al. have synthesized a polymethacrylate with a bistolane mesogenic core directly attached to an azobenzene end group [23,24a]. However, the bistolane moiety has not yet been introduced as the LC core into PLCP materials, which are transparent in the visible region.

In this paper, we describe a synthesis of a new PLCP that exhibits large thermally enhanced photoinduced birefringence as well as its thermally enhanced photoinduced molecular reorientation behavior using LP-365 nm light. We synthesized a polymethacrylate with a photoreactive 4-methoxycinnamoyloxy group directly connected to a bistolane side group (**P1** in Fig. 1). This PLCP showed the largest photoinduced birefringence at the wavelength with non-resonance region among the PLCPs so far. The influence of the degree of the photoreaction and the annealing temperature on the thermally enhanced molecular reorientation behavior was explored in detail. Finally, as a transparent optical application using PLCP films, polarization holographic gratings were fabricated using interference 325 nm light beams in various polarization modes, and their optical properties were characterized. Among **P1**-**P3** films, the gratings of **P1** films exhibited the most efficient diffraction properties due to the largest photoinduced birefringence.

## 2. Experimental section

### 2.1. Materials

Starting materials were used as received from Tokyo Kasei Chemicals and Aldrich Co. Ltd. In addition, we used previously synthesized PLCPs **P2** and **P3** [14,28] Additionally, a polymethacrylate with 4-methoxybistolane side groups (**P4**) was synthesized for the comparison of the photoreaction of the bistolane groups with cinnamate groups in **P3**. The synthetic route for methacrylate monomer with bistolane side groups is outlined in Scheme 1. Monomers **1** and **5** were synthesized according to the literature [28]. The detailed synthetic procedures for **2**-**4**, and **6**-**9**

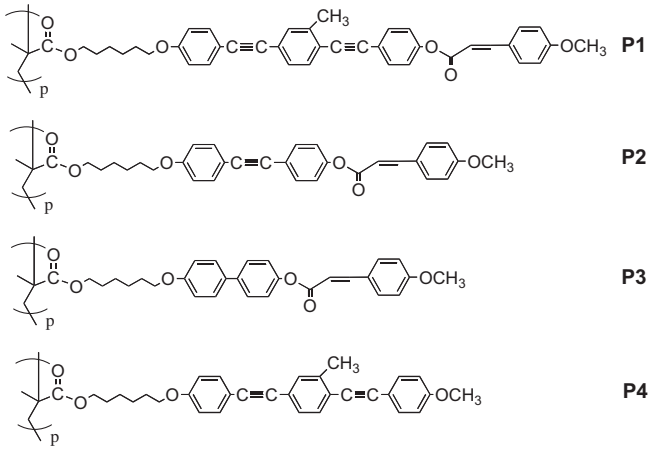


**Fig. 1.** Chemical structures of PLCPs **P1**–**P3**, and **P4**.

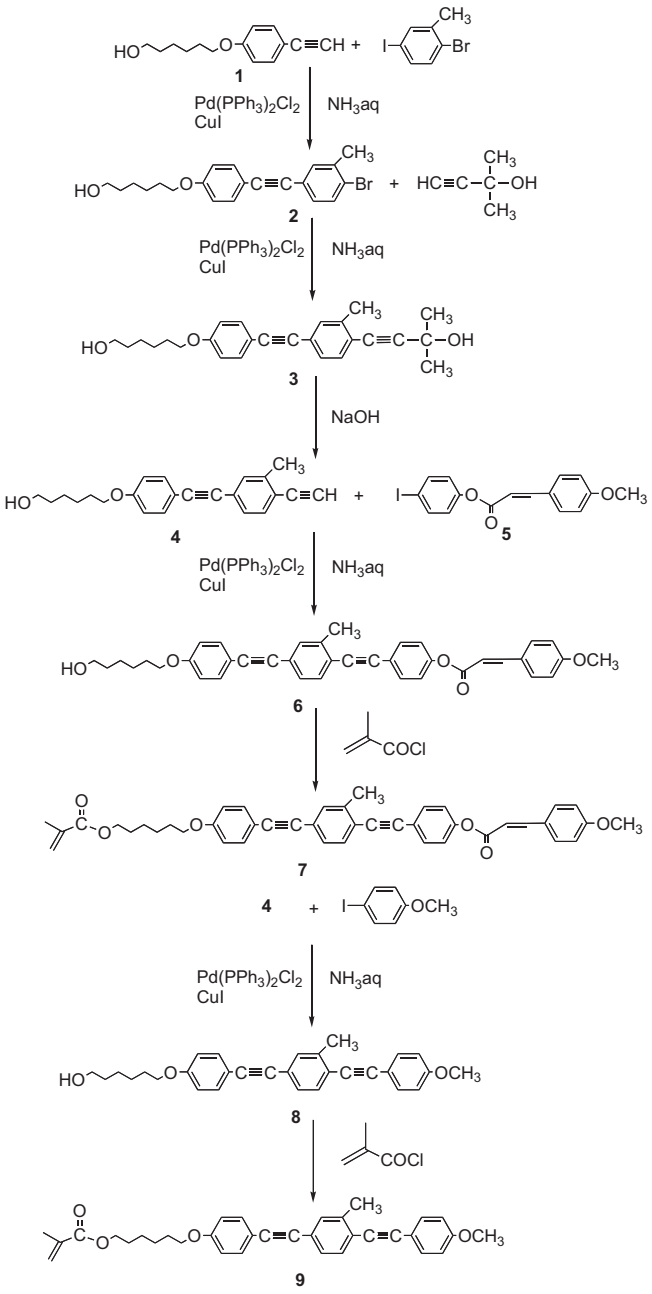


**Scheme 1.** Synthetic route for methacrylate monomers **7** and **9**.

are described in the supporting information. Polymerization was carried out by free radical polymerization of monomers **7** and **9**, in THF, using AIBN as an initiator at 55 °C for one day. Monomer and AIBN concentrations were 10 w/v% and 1.2 mol%, respectively. After the polymerization, we purified the polymers by precipitating them for several times from a THF solution into methanol and

**Table 1**
Molecular weight and thermal properties of the polymers used.

| Polymer | $M_n \times 10^{-4}$ [a] | $M_w/M_n$ | Thermal properties (°C)[b] |
|---|---|---|---|
| P1 | 4.2 | 2.3 | C 114*N* > 300 I |
| P2 | 2.5 | 2.2 | C 66*N* > 300 I |
| P3 | 3.2 | 2.5 | G 105*N* > 300 I |
| P4 | 2.1 | 1.6 | G 96 N 202 I |

[a] Measured by GPC, polystyrene standards, chloroform eluent.
[b] G; glass, C; crystal, N; nematic, I; isotropic. Determined by DSC and POM.

diethyl ether. The synthetic yield was around 50 wt.%. Table 1 summarizes the molecular weight and thermal properties of the polymers.

### 2.2. Photoreaction

Thin polymer films (approximately 150 nm thick) were prepared by spin-coating a methylene chloride solution of polymers (1.0 w/w%) onto quartz or $CaF_2$ substrates. The photoreactions were performed using an ultrahigh-pressure Hg lamp equipped with Glan-Taylor polarizing prisms and a band-pass-filter at 365 nm (FWHM = 10 nm) to obtain LP-365 nm light. This light intensity was 25 $mWcm^{-2}$ at 365 nm. The photoreactivity of the cinnamate and tolane groups of the film was estimated by monitoring the decrease in absorbances at 1639 $cm^{-1}$ (vibration of the cinnamate double bond) and 2200 $cm^{-1}$ (vibration of the carbon–carbon triple bond), respectively, using FT-IR spectroscopy.

### 2.3. Characterization

$^1H$ NMR spectra using a Bruker DRX-500 FT-NMR and FT-IR spectra (JASCO FTIR-410) confirmed the monomers and polymers. The molecular weight of the polymers was measured by GPC (Tosoh HLC-8020 GPC system with a Tosoh TSKgel column; eluent-chloroform) calibrated using polystyrene standards. The thermal properties were examined using a polarization optical microscope (POM; Olympus BHA-P) equipped with a Linkam TH600PM heating and cooling stage in addition to differential scanning calorimetry (DSC; Seiko-I SSC5200H) analysis at a heating and cooling rate of 10 °C$min^{-1}$. The polarization absorption spectra were measured with a Hitachi U-3010 spectrometer equipped with Glan-Taylor polarization prisms. The photoinduced optical anisotropy, $\Delta A$, which was evaluated using polarization absorption spectra, is expressed as Eq. (1):

$$\Delta A = A_{||} - A_{\perp} \quad (1)$$

where $A_{||}$ and $A_{\perp}$ are the absorbances parallel and perpendicular to **E**, respectively. The thermally enhanced molecular reorientation was conducted by annealing an exposed film at an elevated temperature for 5 min. The in-plane order was evaluated using the reorientational order parameter, $S$, which is given in Eq. (2). This equation shows that the reorientation direction is parallel to **E** of the LPUV light for $S > 0$, but perpendicular for $S < 0$.

$$S = \frac{A_{||} - A_{\perp}}{A_{(\mathrm{large})} + 2A_{(\mathrm{small})}} \quad (2)$$

where $A_{||}$ and $A_{\perp}$ are the absorbances parallel and perpendicular to **E**, respectively, while $A_{(large)}$ is the larger value of $A_{||}$ and $A_{\perp}$, and $A_{(small)}$ is the smaller one. Additionally, this equation expresses appropriately the orientation order of the mesogenic groups for both directions. The birefringence ($\Delta n$) of a reoriented film was measured by the Senarmont method at 633 nm [32].

### 2.4. Polarization holography

Polarization holographic grating was recorded with orthogonal linear (OL) exposure using two beams with *s*- and *p*-polarized components [32–34]. Orthogonal circular (OC) exposure consisting of two opposing circular polarization (R- and L-) beams was also carried out. A He–Cd laser (Kinmon Koha, IK3501R-G-S) at a wavelength of 325 nm was used as the light source. The polarization of the laser beams was adjusted by t he use of half- and quarter-wave plates. The optical set-up for polarization holography is illustrated in Fig. 2. After the exposure, the sample film was annealed at elevated temperatures to generate a molecular reorientation. The grating constant ($\Lambda$) was set to 2–15 μm by adjusting the angle ($2\theta$) between two light beams. The holographic gratings were analyzed using a probe beam emitted from a He–Ne laser at a wavelength of 632.8 nm. For first order diffraction, the diffraction efficiency was measured using a photo-detector, and the polarization states were evaluated using a polarizer placed behind the sample plane.

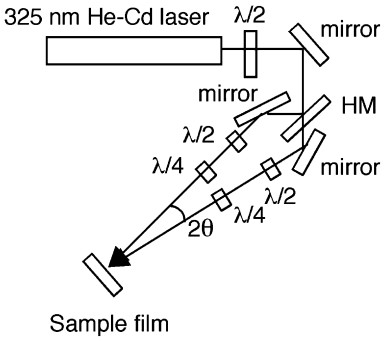


**Fig. 2.** Experimental set up for polarization holography.

## 3. Results and discussion

### 3.1. Synthesis, thermal and spectroscopic properties of PLCPs

PLCP **P1** was synthesized by free radical polymerization in a THF solution. A methyl substituent at the bistolane moiety was introduced to improve solubility of the polymer in common organic solvents, including chloroform, toluene, and DMF [36]. As summarized in Table 1, all polymers revealed a nematic LC phase. The nematic–isotropic transition of **P1**, **P2** and **P3** was above 300 °C and was accompanied by a partial thermal decomposition. In contrast, **P4** exhibited nematic liquid crystalline phase between 96 and 202 °C. DSC curves and POM photographs of the PLCPs are shown in the supporting information (Figs. S1 and S2).

Fig. 3 shows the absorption spectra of **P1**-**P4** films on quartz substrates. The absorption maximum of **P1** was at a longer wavelength than that of **P2** and **P3** due to the conjugation of the bistolane moiety. It contains absorption maxima around 340 nm, and the absorption around 365 nm is large. Additionally, the absorption spectrum of a **P4** film revealed absorption maxima around 320 nm, and it contains moderate absorption around 365 nm. These results indicate that the absorption band of cinnamate group shifted to

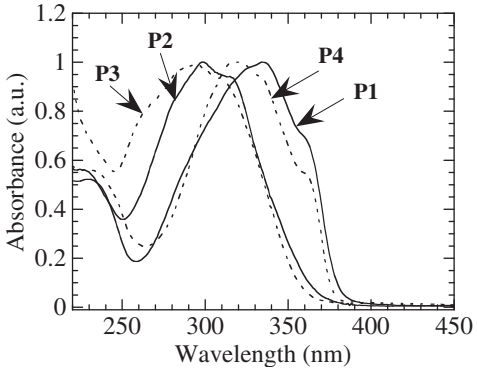


**Fig. 3.** Absorption spectra of **P1**–**P4** films on quartz substrates.

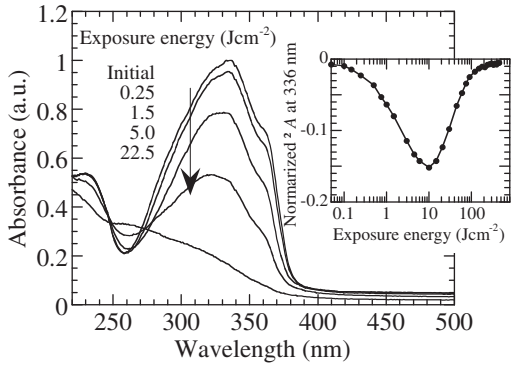


**Fig. 4.** Change in the absorption spectra of a **P1** film upon LP-365 nm light exposure. The inset plots photoinduced optical anisotropies at 336 nm as a function of exposure energy.

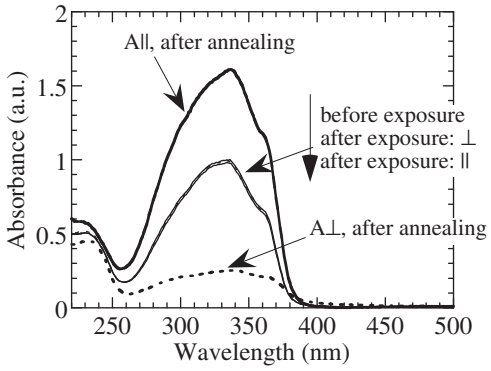


**Fig. 6.** Change in the polarization absorption spectra of a **P1** film before and after irradiating with LP-365 nm light, and after subsequent annealing. Exposure energy and annealing temperatures were 0.15 J cm$^{-2}$ at 230 °C. $A_{\parallel}$ and $A_{\perp}$ indicate absorption parallel and perpendicular to **E** of the LP-365 nm light.

long wavelength due to the bistolane moiety and the absorption band of the bistolane moiety overlaps with that of the cinnamate groups.

### 3.2. Photoreaction of PLCP films

It is well known that exposing a polymeric film with cinnamate side groups to LPUV light leads to an axis-selective [2 + 2] photodimerization and photoisomerization [17,37]. Additionally, the tolane moiety also axis-selectively photoreacted with LPUV light to give photodimerized products [28b,31]. Fig. 4 shows changes in the absorption spectra of a **P1** film when it was exposed to LP-365 nm light. The film became insoluble in organic solvents even though the exposure dose was 0.25 J cm$^{-2}$, suggesting that the photo-cross-linking reaction of the mesogenic side groups occurred at the early stage of the photoreaction. The insets of Fig. 4 plot the photoinduced optical anisotropies at 336 nm as a function of exposure energy. It shows negative optical anisotropy due to the axis-selective photoreaction under LP-365 nm light.

To clarify the detailed photoreaction of the mesogenic side groups of a **P1** film, the photoreaction of the cinnamate and bistolane groups was estimated by FT-IR spectroscopy. Fig. 5a shows change in the FT-IR spectra of a **P1** film. As seen in the figure, the absorption at 1639 cm$^{-1}$ (cinnamate groups) gradually decreased, while the decrease in the absorbance at 2200 cm$^{-1}$ (tolane groups) was very slow. The degree of the photoreaction (DP) of cinnamate ($DP_c$) and bistolane groups ($DP_t$) is plotted in Fig. 5b. It shows that the $DP_c$ gradually increased, whereas the increase in the $DP_t$ was much slower: 95% of the tolane moieties remained when $DP_c$ was 50%. Furthermore, Fig. 5c shows change in the FT-IR spectra of a **P4** film, exhibiting that the photoreaction of the bistolane moiety occurred although larger exposure energy was required as compared to the photoreaction of the cinnamate for **P1**. These results indicate that the photoreaction of the bistolane moieties requires more exposing energy than that of the cinnamate moiety.

### 3.3. Thermal enhancement of the photoinduced optical anisotropy of *P1* film

We have previously reported that a small photoinduced optical anisotropy of the **P2** and **P3** films, which is derived by irradiating with LPUV light, can be reversely enhanced when the exposed films are annealed in the LC temperature range of the material [14,28]. The resultant molecular reorientation was parallel to the **E** of LPUV light and the order parameter was greater than 0.6. This reversibility is due to the self-organization of the non-reacted mesogenic side groups thermally reoriented along the photo-cross-linked groups parallel to **E**, which acted as a photo-cross-linked anchor. The sufficient molecular reorientation was derived when the $DP_c$ was around 1% for **P2**, but more $DP_c$ (10–15%) was required for **P3** [14,28]. This indicates that a small amount of photo-cross-linked anchors with tolane moieties more effectively induced the self-organization of all the mesogenic side groups parallel to **E** than that with biphenyl moieties [28].

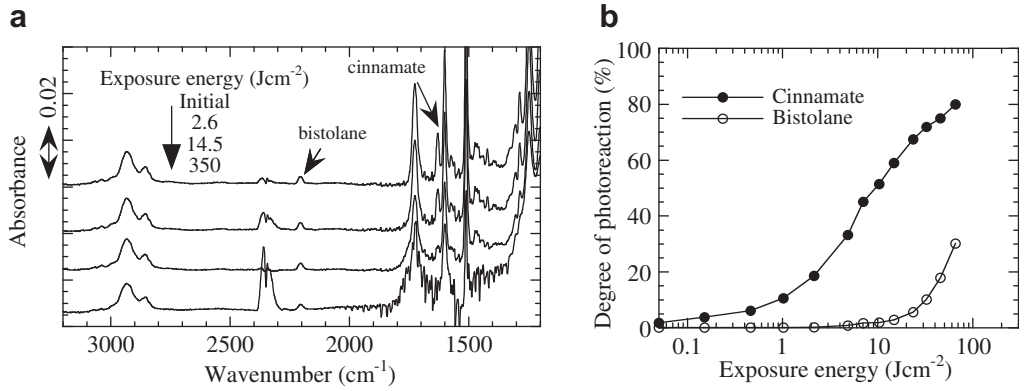


**Fig. 5.** (a) Change in the FT-IR spectra of a **P1** film upon LP-365 nm light exposure. (b) Degree of the photoreaction (DP) of the cinnamate ($DP_c$) and bistolane groups ($DP_t$) of a **P1** film. (c) Change in the FT-IR spectra of a **P4** film upon LP-365 nm light exposure.

**Table 2**
Optical properties of PLCP films with thermally enhanced, photoinduced reorientation.

| Polymer | DP[a] (%) | Annealing temperature[b] (°C) | $S$[c] | $\Delta n$[d] |
|---|---|---|---|---|
| P1 | 2.5 | 230 | 0.64 | 0.34 |
| P2 | 0.8 | 200 | 0.69 | 0.27 |
| P3 | 14.5 | 155 | 0.68 | 0.24 |

[a] Degree of photoreaction.
[b] Annealing for 5 min.
[c] In-plane order parameter at 336 nm for **P1**, and at 314 nm for **P2** and **P3**.
[d] Birefringence at 632.8 nm, as measured by the Senarmont method.

Fig. 6 shows the change in the polarization absorption spectra of a **P1** film before and after irradiating with LP-365 nm light, and after the subsequent annealing, when the maximum thermally enhanced molecular reorientation was obtained. The exposure energy was 0.15 J cm$^{-2}$ ($DP_c = 2.5\%$, $DP_t < 1\%$) and the annealing temperature was 230 °C. After the photoirradiation, the film was insoluble in organic solvents, suggesting the occurrence of photo-cross-linking reaction. The photoinduced negative optical anisotropy after the irradiation with LP-365 nm light was very small ($\Delta A < 0.01$), and reversely amplified by the annealing procedure. This thermal amplification is similar phenomena to that of **P2** and **P3** films. The generated in-plane order parameter, $S$, was +0.64 and the birefringence, $\Delta n$, of **P1** film was 0.34. The maximum generated $S$ and $\Delta n$ values of the **P1**-**P3** films are summarized in Table 2. The $\Delta n$ value of the reoriented **P1** film is the largest among the PLCPs that are transparent in the visible region, although the $S$ value is somewhat smaller than that of **P2** and **P3**. The molecular motion of the long bistolane moieties would be difficult for the sufficient self-organization at elevated temperatures. Despite the smaller $S$ value of the **P1** film, the largest $\Delta n$ value of the reoriented **P1** film is due to the large inherent birefringence and refractive indices of the bistolane moieties. Additionally, the large photoinduced $\Delta n$ (>0.4) had been obtained in polymethacrylate with the bistolane moiety attached with azobenzene side groups [23], although it was a colored material and very large $\Delta n$ value was due to the wavelength measured near the resonance region.

It is worth noting that $DP_c$ required to attain large thermally enhanced molecular reorientation for a **P1** film was much lower than that for **P3** [14]. Additionally, the effective molecular reorientation for the **P2** film was achieved at an early stage of the photoreaction [28]. These results indicate that a small amount of axis-selective, photo-cross-linked mesogenic groups with (bis)tolane moieties parallel to **E** effectively act as the photo-cross-linked anchors. Further detailed results are discussed in the following section.

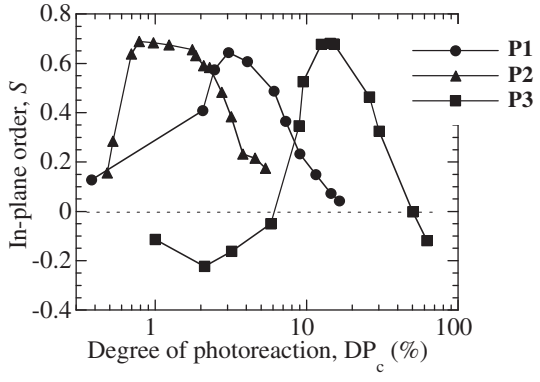


**Fig. 7.** Thermally enhanced $S$ values of **P1** (at 336 nm), and **P2** and **P3** (at 314 nm) films as a function of $DP_c$. The annealing temperatures were 230 °C for **P1**, 200 °C for **P2** and 155 °C for **P3**.

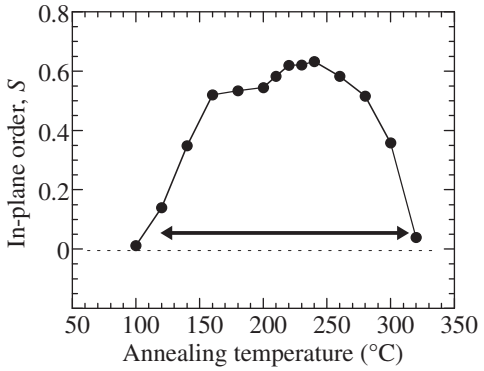


**Fig. 8.** Thermally enhanced $S$ values for **P1** (at 336 nm) films as a function of the annealing temperature. $DP_c$ was 2.5%. Arrow shows the LC temperature range of the PLCP.

### 3.4. Effect of the degree of photoreaction on molecular reorientation

The DP influenced thermally enhanced molecular reorientation behavior. Fig. 7 plots the thermally enhanced $S$ values of **P1** films as a function of $DP_c$, in which films were exposed to LP-365 nm light and subsequently annealed. For comparison, the thermally enhanced $S$ values of **P2** and **P3** films are also plotted. The annealing temperatures were 230 °C for **P1**, 200 °C for **P2** and 155 °C for **P3**.

For **P1**, sufficient molecular reorientation parallel to **E** ($S > +0.6$) was observed when $DP_c$ was around 2.5–4.5%. The generated maximum $S$ values decreased as the $DP_c$ further increased and the molecular reorientation did not occur when the $DP_c$ was greater than 10%. The molecular mobility for the self-organization reduced due to the large amount of photo-cross-linked products. For **P2**, smaller amount of photoreaction was required for the maximum molecular reorientation parallel to **E**, where the required $DP_c$ was around 1%. In contrast, larger amount ($DP_c = 10–15\%$) of photoreaction was needed for the sufficient molecular reorientation parallel to **E** for **P3** films, while molecular reorientation perpendicular to **E** was observed when the $DP_c$ was several %. In this case, small amount of photoproducts act as impurities to reduce the liquid crystalline property parallel to **E** of LPUV light, resulting in the thermally enhanced self-organization perpendicular to **E**. This

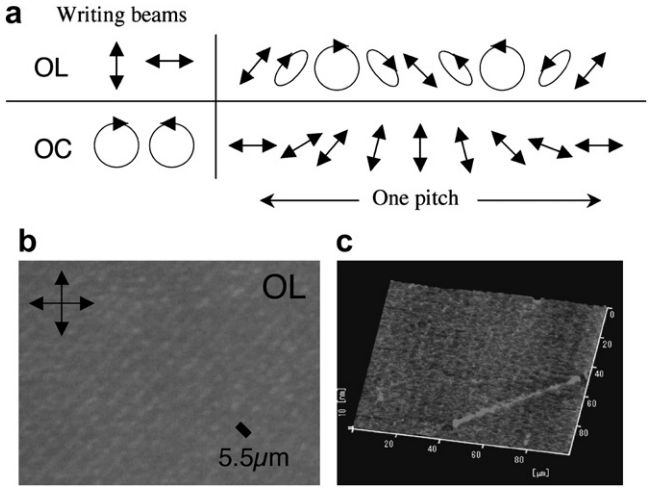


**Fig. 9.** (a) Polarization modulation of the interference light beams under OL and OC conditions. (b) POM photographs of the polarization gratings of **P1** films with OL condition. The arrows show the direction of the polarizers. (c) AFM image of the gratings of **P1** films with OL condition.

**Table 3**
The fabrication conditions and optical properties of polarization gratings.

| Polymer | Two beams[a] | Exposure energy[a] (mJ cm$^{-2}$) | $\eta$ (%)[b] | $\Delta n$[c] |
|---|---|---|---|---|
| P1 | OL | 40 | 1.5 | 0.33 |
| P1 | OC | 40 | 2.8 | 0.32 |
| P2 | OL | 22 | 1.0 | 0.27 |
| P2 | OC | 22 | 1.9 | 0.26 |
| P3 | OL | 400 | 0.7 | 0.23 |
| P3 | OC | 400 | 1.3 | 0.23 |

[a] Film thickness 150 nm. Exposure was by 325 nm He-Cd laser.
[b] First-order diffraction efficiency at 633 nm. The Incident beam was linearly polarized.
[c] Birefringence at 632.8 nm.

thermal enhancement perpendicular to **E** was observed in azobenzene-containing LC polymers and PLCPs with H-bonded mesogenic side groups [38–40]. For **P1** and **P2**, thermal enhancement perpendicular to **E** did not occur. A small amount of photoreacted side groups parallel to **E** act as the photo-cross-linked anchor for the self-organization rather than acting as the impurities. The thermally enhanced molecular reorientation of the (bis) tolane moieties parallel to **E** is initiated by a small amount of photoreaction of the cinnamate end groups. Additionally, the larger required $DP_c$ for the effective orientation of the **P1** film than that of **P2** could be due to the methyl substituent at the bistolane moiety. A similar phenomenon has been observed for **P2** analogues, when the tolane moiety had a methyl substituent [28b]

### 3.5. Effect of the annealing temperature on molecular reorientation

The annealing temperature also influenced thermally enhanced molecular reorientation, as plotted in Fig. 8. Here, $DP_c$ for **P1** was 2.5%. The figure shows that the thermal amplification of the molecular reorientation occurred when annealing temperature was in the LC temperature range of the material. This is quite similar to the case of other PLCP films that exhibited thermal amplification of the photoinduced optical anisotropy based on a photo-cross-linked anchor.

### 3.6. Polarization holography

Polarization gratings were recorded using two beam interferometry with OL and OC beams using **P1**-**P3** films. In these recording conditions, light intensity is not modulated, but the polarization of the interferometric light beams is, as illustrated in Fig. 9a. These holographic recordings induce a periodic molecular

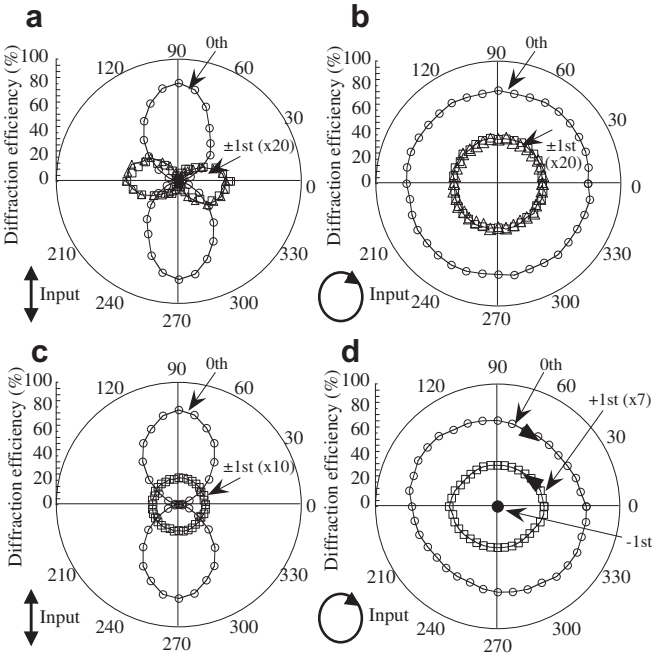


**Fig. 11.** Polarization analysis of the beams diffracted from the polarization gratings of the **P1** film. (a) Grating by OL, linear incident polarization. (b) Grating by OL, R-circularly polarized incident beam. (c) Grating by OC, linear incident polarization. (d) Grating by OC, R-circularly polarized incident beam.

reorientation of the PLCP films according to the polarization modulation direction, which form the pure polarization gratings. The grating constant was set to 2–15 μm by adjusting the angle of two beams [41].

Fig. 9b shows POM photographs of fabricated **P1** gratings with 40 mJ cm$^{-2}$ doses of OL beam when the grating constant was 11 μm. It reveals that a bright area appears every 5.5 μm, which corresponds to the half pitch of the grating constant. A bright area implies that the uniaxial molecular reorientation and the neighboring orientation directions are orthogonal to each other. AFM image revealed that the height of the surface relief formation was less than 3 nm as shown in Fig. 9c, due to the uniform light intensity of the polarization holography. The grating fabricated with the OC beam showed a similar results (Fig. S3). Thus, polarization holographic recording was successfully fabricated on a **P1** film for both recording conditions. Additionally, polarization grating of **P2** and **P3** films were also fabricated. Table 3 summarizes

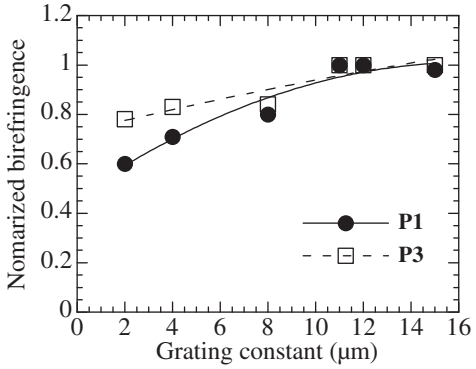


**Fig. 10.** Dependence of the induced birefringence on the grating constant for **P1** and **P3** films. The graph is normalized at maximum birefringence in polarization holograms fabricated with OL beam.

| Writing | Reading | Polarization (DE %) +1st order | Polarization (DE %) -1st order |
|---|---|---|---|
| OL | ↕ | ↔ (1.5) | ↔ (1.5) |
| | ↻ | ↻ (1.4) | ↻ (1.5) |
| OC | ↕ | ↻ (2.8) | ↻ (2.7) |
| | ↻ | ↻ (5.2) | Invisible |
| | ↺ | Invisible | ↻ (5.3) |

**Fig. 12.** Summary of the polarization states of the ±1st order diffracted beams on polarization gratings using **P1** film. The diffraction efficiencies (DEs) of each diffraction beam appear in parentheses.

the fabrication conditions and optical properties of polarization gratings of **P1**-**P3** films when the maximum diffraction efficiency was obtained. The $\Delta n$ values were calculated by the theoretical consideration using the value of the diffraction efficiency [35b]. It shows that the energy required for fabricating satisfactory gratings of **P1** and **P2** films was much lower than for **P3** films because of the low exposure energy required for the effective molecular reorientation. Additionally, the $\Delta n$ values generated were similar to those estimated from the uniaxially molecular-reoriented films for all the gratings, since polarization holography induced the efficient molecular reorientation. Furthermore, due to its larger $\Delta n$ values of reoriented **P1** film, the diffraction efficiency was the highest among **P1**-**P3** films.

To evaluate the resolution of the polarization gratings, the influence of the grating constant on the polarization holography was investigated [41]. Fig. 10 plots the induced birefringence at 632.8 nm of **P1** and **P3** films for various grating constant, where the induced $\Delta n$ was normalized at a maximum value. As the grating constant becomes larger, the induced birefringence also becomes larger until it is approximately saturated at a grating constant of 11 μm in both materials. It seems that the resolution of **P1** might be lower than that of **P3**, when the grating constant was small. Because **P1** contains elongated and rigid mesogenic side groups, thermally enhanced reorientation process possesses a limitation for the sufficient periodical molecular orientation.

One of the features of the polarization gratings is the conversion of the polarization of the diffracted beams. Fig. 11a–d show polar-plots of the 0th and ±first-order diffracted laser beams for **P1** polarization gratings, which represent the optical intensity distribution along a polarization azimuth angle as polarization states. The characteristics of the fabricated polarization gratings and the first-order diffraction efficiencies are shown in Fig. 12. For the grating fabricated with OL beams, the polarization of the diffracted beams was rotated by 90 deg, when the linearly polarized probe beam was used as plotted in Fig. 11a. This grating reversed the rotation direction of the ±first-order diffracted beams, when the probe beam was circularly polarized (Fig. 11b). For the grating of fabricated with OC beams, the polar plot of Fig. 11c shows that the circularly polarized, diffracted beams with opposite circular rotations are obtained for a linearly polarized probe beam. Interestingly, when the probe was R-circularly polarized, only the +first order diffraction beam was observed and the rotation direction was reversed, but the -first order was invisible, as plotted in Fig. 11d. Furthermore, the diffraction efficiency of the +first order beam was twice that of a linearly polarized probe beam. These experimental results are consistent with the theoretical predictions for pure polarization gratings [33–35].

## 4. Conclusion

A thermally enhanced in-plane molecular reorientation with large birefringence was investigated in a thin PLCP (**P1**) film comprised of a 4-methoxycinnamoyloxy group directly connected with a bistolane moiety. Based on the axis-selective photoreaction of the cinnamate groups, the generated in-plane reorientational order was greater than 0.6, and the birefringence was $\Delta n = 0.34$ at 633 nm. This is the largest $\Delta n$ value for thermally enhanced molecular reorientation for materials transparent in the visible region. In addition, we have demonstrated optical device applications, such as polarization holography. Due to the larger generated birefringence, efficient diffraction efficiency was obtained. Further applications using **P1** films for thinner birefringent devices is currently under investigation.

## Acknowledgments

This work was partially supported by a grant-in-aid of Scientific Research in Priority Areas “New Frontiers in Photochromism (No. 471)” from the Ministry of Education, Culture, Sports, Science and Technology (MEXT), and a grant-in-aid of Scientific Research B (No. 21350129) and S (No. 21225006) from the Japan Society for the Promotion of Science.

## Appendix. Supplementary material

Supplementary data associated with this article can be found, in the online version, at doi:10.1016/j.polymer.2010.04.043.

## References

[1] (a) Shibaev VP, Kostromin SG, Ivanov SA. In: Shibaev VP, editor. Polymers as electroactive and photooptical media. Berlin: Springer; 1996. p. 37–110;
(b) MacArdle CB. In: MacArdle CB, editor. Applied photochromic polymer systems. New York: Blackie; 1991. p. 1–30;
(c) Krongauz V. In: MacArdle CB, editor. Applied photochromic polymer systems. New York: Blackie; 1991. p. p121–73.
[2] (a) Ichimura K. Chem Rev 2000;100:1847–73;
(b) Natansohn A, Rochon P. Chem Rev 2002;102:4139–76;
(c) Ikeda TJ. Mater Chem 2003;13:2037–57.
[3] O'Neill M, Kelly SM. J Phys D Appl Phys 2000;33:R67–84.
[4] Seki T. In: Nalwa HS, editor. Handbook of photochemistry and photobiology, vol. 2. Stevenson Ranch, CA: American Sci Publishers; 2003. p. 435–65.
[5] (a) Anderle K, Birenheide R, Eich M, Wendrorff JH. Makromol Chem Rapid Commun 1989;10:477–83;
(b) Shi Y, Steier WH, Yu L, Chen M, Dalton LR. Appl Phys Lett 1991;59:2935–7.
[6] Kawatsuki N, Ono H. In: Nalwa HS, editor. Organic electronics and photonics, vol. 2. Stevenson Ranch, CA: American Sci Publishers; 2007. p. 301–44.
[7] Schadt M, Schmitt K, Kozinkov V, Chigrinov V. Jpn J Appl Phys 1992;31:2155–64.
[8] Schadt M, Seiberle H, Schuster A. Nature 1994;381:212–5.
[9] Gibbons WM, Shannon PJ, Sun ST, Swetlin BJ. Nature 1991;351:49–50.
[10] (a) Wu Y, Demachi Y, Tsustusmi O, Kanazawa A, Hisono T, Ikeda T. Macromolecules 1998;31:4457–63;
(b) Wu Y, Demachi Y, Tsustusmi O, Kanazawa A, Hisono T, Ikeda T. Macromolecules 1998;31:1104–8.
[11] Han M, Ichimura K. Macromolecules 2001;34:90–8.
[12] Natansohm A, Rochon P, Pézolet M, Audet P, Brown D, To S. Macromolecules 1994;27:2580–5.
[13] (a) Kawatsuki N, Takatsuka H, Yamamoto T, Sangen O. J Polym Sci Part A Polym Chem 1998;36:1521–6;
(b) Kawatsuki N, Ono H, Takatsuka H, Yamamoto T, Sangen O. Macromolecules 1997;30:6680–2.
[14] Kawatsuki N, Goto K, Kawakami T, Yamamoto T. Macromolecules 2002;35:706–13.
[15] (a) Jackson PO, O'Neill M, Duffy WL, Hindmarsh P, Kelly SM, Owen GJ. Chem Mater 2001;13:694–703;
(b) Bergmann G, Jackson PO, Hogg JHC, Stirner T, O'Neill M, Duffy WL, et al. Appl Phys Lett 2005;87:061914.
[16] Trajkovska A, Kim C, Marchall KL, Mourey TH, Chen SH. Macromolecules 2006;39:6983–9.
[17] (a) Xiao S, Lu X, Lu Q, Su B. Macromolecules 2008;41:3884–92;
(b) Xiao S, Lu X, Lu Q. Macromolecules 2007;40:7944–50;
(c) Zhang Q, Bazuin CG, Barret CJ. Chem Mater 2008;20:29–31.
[18] Barachevsky VA. Proc SPIE 1991;1559:184–93.
[19] Kawatsuki N, Kawakami T, Yamamoto T. Adv Mater 2001;13:1337–9.
[20] Kawatsuki N, Matsuyoshi K, Hayashi M, Takatsuka H, Yamamoto T. Chem Mater 2000;12:1549–55.
[21] Gerhard P. In: Demus D, Goodby J, Gray GW, Spiess HW, editors. Handbook of liquid crystals, vol. 2A. New York: Wiley-VCH; 1998. p. 128–41.
[22] Ye F, Orita A, Yaruba J, Hamada T, Otera J. Chem Lett 2004;33:528–9.
[23] (a) Okano K, Shishido A, Ikeda T. Adv Mater 2006;18:523–7;
(b) Okano K, Tsutsumi O, Shishido A, Ikeda T. J Am Chem Soc 2006;128:15368–9.
[24] (a) Okano K, Shishido A, Ikeda T. Macromolecules 2006;39:145–52;
(b) Yoneyama S, Yamamoto T, Tsutsumi O, Kanazawa A, Shiono T, Ikeda T. Macromolecules 2002;35:8751–8.
[25] (a) Shishido A, Ishiguro M, Ikeda T. Chem Lett 2007;36:1146–7;
(b) Ishiguro M, Sato D, Shishido A, Ikeda T. Langmuir 2007;23:332–8.
[26] Yu H, Kobayashi T, Ge Z. Macromol Rapid Commun 2009;30:1725–30.
[27] Kitani Y, Kitamura C, Yoneda A, Kawatsuki N. Mol Cryst Liq Cryst 2005;443:181–9.
[28] (a) Kawatsuki N, Fujii Y, Kitamura C, Yoneda A. Chem Lett 2006;35:52–3;
(b) Kawatsuki N, Yamashita A, Fujii Y, Kitamura C, Yoneda A. Macromolecules 2008;41:9715–21.

[29] Okano K, Mikami Y, Yamashita T. Adv Funct Mater 2009;15:3804–8.
[30] Michinobu T, Noguchi H, Fujii N, Tokita M, Watanabe J, Shigehara K. Chem Lett 2008;37:356–7.
[31] Obi M, Morino S, Ichimura K. Chem Mater 1999;11:1293–301.
[32] El-Hosseiny FJ. Opt Soc Am 1975;65:1279–82.
[33] (a) Fleck B, Helgert M, Wenke LJ. Opt A Pure Appl Opt 2000;2:16–20;
(b) Helgert M, Fleck B, Wenke L. Opt Commun 2000;177:95–104.
[34] Cipparrrone G, Mazzulla A, Blinov LM. J Opt Soc Am B 2002;19:1157–61.
[35] (a) Kawatsuki N, Hasegawa T, Ono H, Tamoto T. Adv Mater 2003;15:991–4;
(b) Ono H, Emoto A, Kawatsuki N, Hasegawa T. Appl Phys Lett 2003;94:1359–61.
[36] (a) Broer DJ, Heynderickx I. Macromolecules 1990;23:2474–7;
(b) Hikmet RA, Lub J, Higgins JA. Polymer 1993;34:1736–40.
[37] Ichimura K, Akita Y, Akiyama H, Kudo K, Hayashi Y. Macromolecules 1997;30:903–11.
[38] Kidowaki M, Fujiwara T, Ichimura K. Chem Lett 1999:641–2.
[39] Stumpe J, Fischer T, Rutloh M, Rosenhauer R, Meier JG. Proc SPIE 1999;3800:150–63.
[40] (a) Uchida E, Kawatsuki N. Polymer 2006;47:2322–9;
(b) Uchida E, Kawatsuki N. Macromolecules 2006;39:9357–64.
[41] Emoto A, Matsumoto T, Yamashita A, Shioda T, Ono H, Kawatsuki N. Appl Phys Lett 2009;106:073505.